

# Learning What *NOT* to Count

Adriano D’Alessandro  
Simon Fraser University  
acdaless@sfu.ca

Ali Mahdavi-Amiri  
Simon Fraser University  
amahdavi@sfu.ca

Ghassan Hamarneh  
Simon Fraser University  
hamarneh@sfu.ca

## Abstract

*Few/zero-shot object counting methods reduce the need for extensive annotations but often struggle to distinguish between fine-grained categories, especially when multiple similar objects appear in the same scene. To address this limitation, we propose an annotation-free approach that enables the seamless integration of new fine-grained categories into existing few/zero-shot counting models. By leveraging latent generative models, we synthesize high-quality, category-specific crowded scenes, providing a rich training source for adapting to new categories without manual labeling. Our approach introduces an attention prediction network that identifies fine-grained category boundaries trained using only synthetic pseudo-annotated data. At inference, these fine-grained attention estimates refine the output of existing few/zero-shot counting networks. To benchmark our method, we further introduce the FGTC dataset, a taxonomy-specific fine-grained object counting dataset for natural images. Our method substantially enhances pre-trained state-of-the-art models on fine-grained taxon counting tasks, while using only synthetic data. Code and data to be released upon acceptance.*

## 1. Introduction

Counting the occurrences of specific objects in an image is a critical task with applications across diverse fields, from inventory management and wildlife monitoring to traffic analysis and medical imaging. However, supervised object counting methods require expensive annotated data, which is difficult and costly to obtain, especially for images with large crowds and occlusion. This dependency on extensive annotations creates a significant barrier to developing counting models for novel real-world applications, limiting their practical use across many scenarios. Recent advances in few-shot and zero-shot [6, 28, 31, 33] counting methods have reduced the need for exhaustive manual annotation by allowing class definition at inference time, making object counting significantly more scalable. Typically, these methods are trained on broad-category counting datasets like



Figure 1. **Overview.** Previous few-shot and zero-shot counting methods tend to overcount in fine-grained scenarios. Our approach addresses this limitation using synthetic data.

FSC147 [25], where images are grouped into general categories such as *birds*, *bricks*, or *boxes*. While effective in general contexts, these methods struggle to differentiate between multiple object categories within a single scene [18]. Further, these methods fail entirely in fine-grained scenarios where objects from a specific subcategory must be differentiated from multiple visually similar categories such as in Figure 1. This limitation underscores the need for data-efficient solutions capable of tackling fine-grained object taxon counting, where subtle distinctions between categories are crucial and existing methods fall short.

In this work, we introduce the problem of *annotation-free fine-grained object taxon counting*. This task involves distinguishing between visually similar object categories, such as subspecies or cultivars, that often co-exist within the same image. However, in line with previous annotation-free approaches [5, 10], our method operates under the constraint that no manual annotations are available.

Our approach is based on two key insights. First, generative models, such as Stable Diffusion [22], generate realistic images of fine-grained categories, although they struggle to depict closely related categories within a single image [3]. Second, we find that the cross-attention maps produced during image synthesis [9] localize the generated objects while ignoring the background. These attention maps serve as pseudo-annotations that can guide the training of networks



Figure 2. **FGTC Dataset**. Sample images from our fine-grained counting dataset, showcasing three main categories: peppers, wildflowers, and waterfowl. Each main category is divided into fine-grained subcategories. The dataset includes crowded, diverse images with multiple distinct object types in each scene, highlighting the variety and complexity of the data.

to learn fine-grained distinctions without manual labeling.

Building on these insights, our method uses diffusion models to generate synthetic images and attention maps for specific fine-grained categories, which are then used to train an attention-guidance model. This model learns to focus on target objects (‘what to count’) while filtering out similar but irrelevant ones (‘what not to count’). Given an input image, the attention-guidance model accurately highlights regions containing only the target fine-grained category. By applying these attention maps to pre-existing object counting networks, we exclude objects we do not wish to count, enabling fine-grained counting on demand.

To benchmark our approach, we introduce FGTC (See: Fig. 2), the first dataset focused on fine-grained object taxon counting across diverse object categories. Designed specifically for limited-data methods that avoid manual annotation for fine-grained counting, FGTC includes a test set of 931 images, providing a benchmark for models adapted to handle fine-grained distinctions in zero/few-shot setting.

In summary, our contributions are as follows:

- A novel annotation-free method leveraging synthetic data from latent diffusion models for fine-grained counting.
- A generic method for adapting pre-trained object counting networks to perform fine-grained counting via attention prediction and attention-based region isolation.
- The FGTC benchmark dataset for fine-grained counting.

## 2. Related Work

Few-shot counting was first introduced with the FSC147 dataset [25], where methods [2, 6, 21, 28] use patch-based exemplars to identify and count target objects in new im-

ages. Similar to our method, DAVE [21] introduces a filtering strategy for reducing false positives in few-shot counting. However, while DAVE relies on spectral clustering, our approach learns to filter using synthetic data. Moreover, as shown in Figure 3, DAVE fails entirely on fine-grained counting, despite its filtering mechanism.

Zero-shot counting [31–33] extends this paradigm by defining classes through text-based prompts, removing the need for image exemplars and enabling flexible, text-driven counting. Additionally, unsupervised and weakly supervised methods [5, 7, 11, 26] have been explored for single-category object counting.

**Learning from Synthetic Images.** Synthetic image data generated by latent diffusion models is increasingly explored as a solution for real-world challenges [8, 23, 27]. Closest to our approach, AFreeCA [5] uses weak signals from synthetic images for single-category, unsupervised object counting. In contrast, our work extends this concept to multi-class fine-grained categories, using synthetic data to adapt pre-trained networks to fine-grained counting.

**Fine-Grained Image Analysis.** Previous work on fine-



Figure 3. **Overcounting**. DAVE [21] employs a filtering strategy to reduce false positives but fails on fine-grained categories, resulting in overcounting—illustrated in these images of peppers

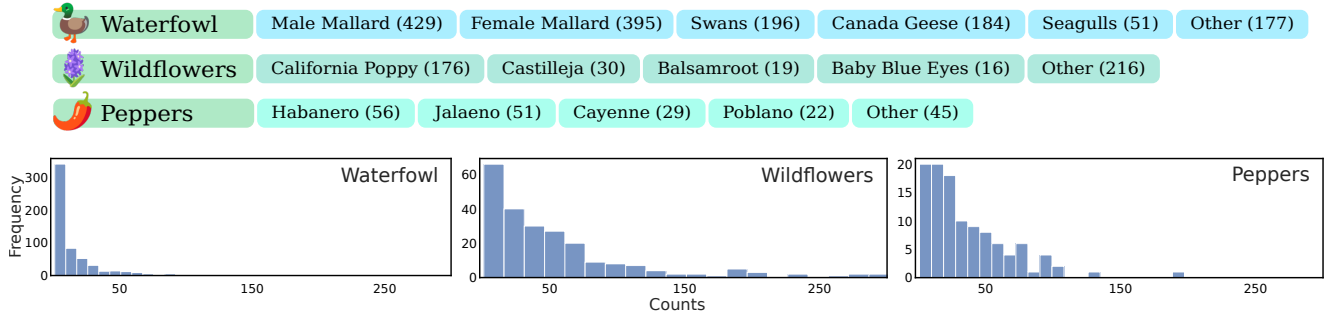


Figure 4. **FGTC Overview.** (Top) The dataset contains three broad categories, each divided into fine-grained subcategories. We display the number of images containing at least one instance of each subcategory. (Bottom) The distribution of object counts across the dataset.

Top-Level Categories	Subcategories per Image					
	1	2	3	4	5	6
Waterfowl	62	303	135	51	24	4
Wildflowers	25	210	4	0	0	0
Peppers	56	33	14	4	5	0

Table 1. **Subcategories per Image.** The majority of images contain 2+ subcategories per image, highlighting the data complexity.

grained image recognition has explored various approaches, each emphasizing different details. Taxonomy-based fine-grained analysis, as seen in datasets like CUB-200 [29] and Oxford Flowers [19], categorizes images based on shared taxonomies with subtle inter-category differences. Our work builds on this by extending taxonomy-based analysis to annotation-free object counting in crowded scenes.

Attribute-based analysis, such as referring object detection [13, 14, 30], focuses on identifying objects with *fine-grained attributes* like color or behavior. The REC-8K dataset [4] presents a problem similar to our work that involves referred-expression counting, allowing for distinctions between simple categories and basic attributes, such as color (e.g., *blue car* vs. *red car*). However, REC-8K’s training and test sets share significant category overlap (75%), focusing primarily on capturing novel attributes for established categories. In contrast, our work aims to extend to novel *fine-grained categories* without requiring manual annotation, addressing a previously unexplored challenge with broad applications across multiple fields.

### 3. Fine-Grained Taxon Counting Dataset

Fine-grained object taxon counting involves distinguishing between closely related categories within a shared taxonomic class, presenting a unique set of challenges. Unlike broad-category counting, which identifies all objects of a general type (e.g., “birds” or “peppers”), this approach requires models to differentiate between visually similar sub-

categories. This level of nuanced categorization is essential in fields like ecology, where precise counts of species within a habitat can inform conservation efforts, or agriculture, where distinguishing between types of crops impacts resource allocation and pest management strategies.

To address the need for fine-grained object taxon counting, we introduce the FGTC dataset, a benchmark uniquely combining fine-grained recognition with multi-class counting. Unlike previous datasets, FGTC includes high-density images containing multiple subcategories of objects within the same taxonomic class, closely mirroring real-world conditions. Sample images in Fig. 2 illustrate the dataset’s complexity, making FGTC a valuable resource for evaluating a counting model’s ability to generalize to fine-grained distinctions across taxonomic classes.

#### 3.1. Dataset Composition

The FGTC dataset consists of three taxonomic categories, outlined in Fig. 4, designed to test counting models on differentiating similar objects in densely populated scenes.

- **Waterfowl:** Includes Swans, Canadian Geese, Seagulls, Male Mallard Ducks, and Female Mallard Ducks, reflecting species that commonly co-occur in natural habitats.
- **Wildflowers:** Contains species like Balsamroot, California Poppies, Castilleja, and Baby Blue Eyes, reflecting diverse natural environments.
- **Peppers:** Cultivars such as Habanero, Cayenne, Poblano, and Jalapeno, which are relevant for quality control and inventory management in food systems applications.

The dataset also includes images with additional, infrequently occurring subcategories labeled as “other” in Fig. 4. These less common subcategories are grouped together and treated as a single background class.

#### 3.2. Data Collection and Annotation Process

To construct the FGTC dataset, we collected images under Creative Commons licenses from Flickr, Unsplash, and Pexels, using targeted search queries based on each object’s subcategory name. Selection criteria focused on maintain-

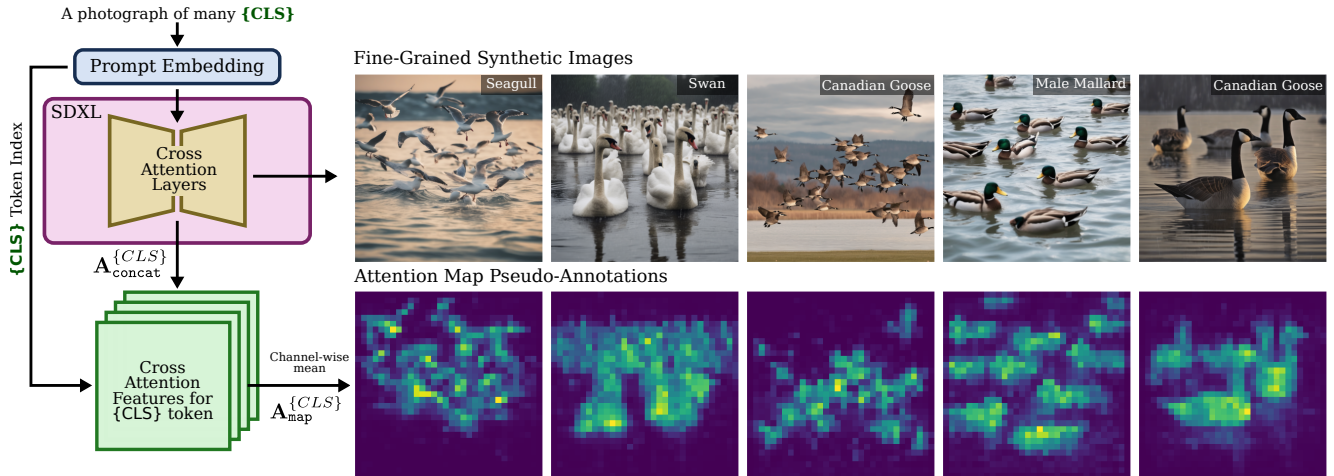


Figure 5. **Synthetic Data Generation.** Our methodology leverages Stable Diffusion XL to generate dense scenes with objects from a single fine-grained category, utilizing attention maps produced during synthesis to localize objects of interest.

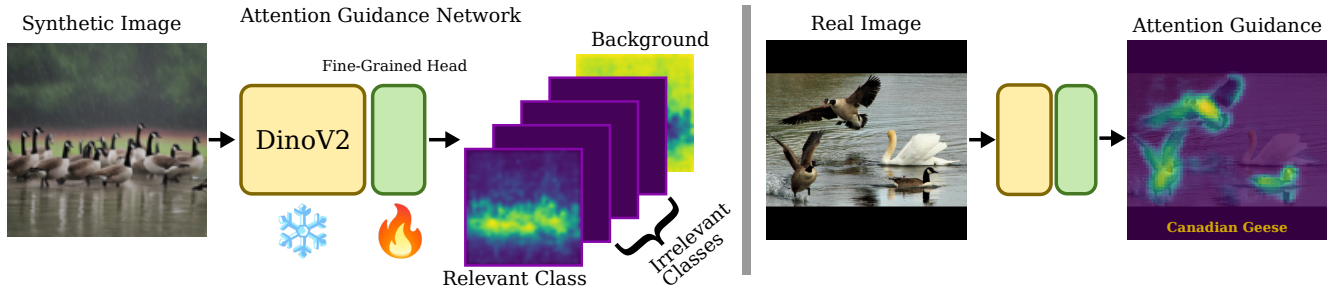


Figure 6. **Methodology.** Our approach begins by using synthetic image and semantic attention map pairs to fine-tune an attention guidance network (left). This trained network is then applied to generate attention guidance maps for real images (right). Observe how the swan is correctly removed from the Attention Guidance map, which only attends to Canadian Geese.

ing crowd density, visual variability, and the presence of multiple subcategories within each image, creating realistic scenarios for fine-grained counting. In Tab. 1, we provide an overview of the image distribution by the number of relevant fine-grained subcategories present, noting that nearly all selected images contain two or more subcategories.

To standardize resolution, all images were resized to a maximum of 2,048 pixels on the longest side. For annotations, we provide the object counts along with point labels applied to the approximate center of each object within an image, with each label specifying the fine-grained category.

### 3.3. Dataset Split and Evaluation

To support few/zero-shot counting objectives, FGTC includes a test set of 931 images and three taxonomic categories. This setup focuses on evaluating models trained without manual annotations from fine-grained categories, assessing their ability to generalize to unseen classes.

Overall, FGTC addresses a critical gap and serves as a novel benchmark for evaluating fine-grained object count-

ing capabilities, challenging models to distinguish subtle inter-class variations within densely populated scenes.

## 4. Methodology

Fine-grained object counting is a challenging task, particularly in crowded scenes where objects from similar categories may be present together and they need to be distinguished. To address these challenges, we rely on the following insights: (1) synthetic data could be a valuable resource for fine-grained counting tasks, (2) cross-attention maps extracted from latent diffusion models can be used as fine-grained annotations, and (3) pre-existing counting models often perform well for generic object counting and could be adapted to fine-grained scenarios where they underperform.

In the following section, we present an annotation-free method that leverages synthetic data from latent diffusion models. By generating high-quality synthetic images and extracting cross-attention maps, we create pseudo-annotated attention maps for category-specific spatial guidance. We then demonstrate how to use these maps to train

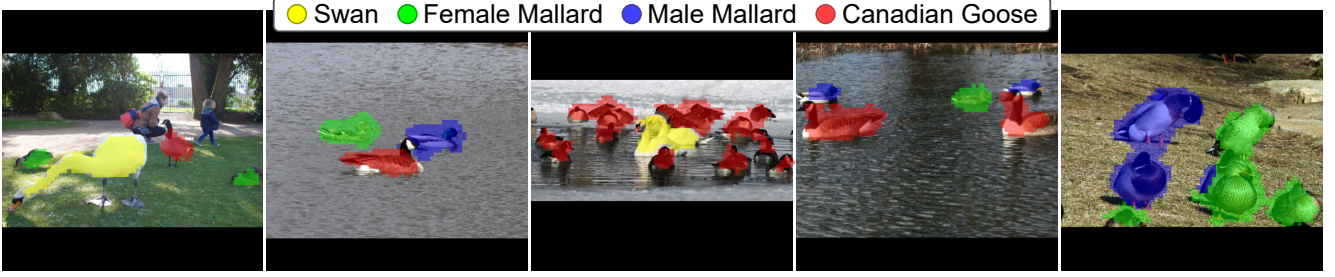


Figure 7. **Attention Guidance.** We visualize the attention guidance on real images by using a simple threshold to produce semantic masks, demonstrating that our attention guidance strategy focuses on the correct objects, even when multiple similar objects are present.

networks for fine-grained attention guidance, allowing us to adapt and significantly improve pre-trained object counting models for the fine-grained taxon counting task.

#### 4.1. Fine-grained Synthetic Data

Creating annotated data for fine-grained categories requires considerable manual effort, making it impractical at scale. To address this, we utilize Stable Diffusion XL (SDXL) [22] as a synthetic data generation tool and find it capable of producing high-quality, realistic images containing multiple objects from specific fine-grained categories, as seen in Figure 5. This capability allows us to generate a diverse set of synthetic images that closely resemble real-world scenes. Our approach further leverages the internal cross-attention mechanism of SDXL to generate fine-grained attention annotations for these synthetic images:

$$(x^{\text{syn}}, \mathbf{A}_{\text{map}}^{\{\text{CLS}\}}) \leftarrow \text{SDXL}(\text{prompt}^{\{\text{CLS}\}}), \quad (1)$$

where  $x^{\text{syn}}$  is a synthetic image containing objects from category  $\{\text{CLS}\}$ ,  $\text{prompt}^{\{\text{CLS}\}}$  is a text prompt describing the objects, and  $\mathbf{A}_{\text{map}}^{\{\text{CLS}\}}$  is a semantic attention heat map that localizes the objects in  $x^{\text{syn}}$ . As illustrated in Fig. 5, the process begins by tokenizing the prompt and generating embeddings for each token, which are then fed into SDXL’s cross-attention layers during generation. Our objective is to extract the cross-attention maps that capture the interactions between the synthetic image features and the specific token for the fine-grained category  $\{\text{CLS}\}$ .

We define the cross-attention map from SDXL layer  $l$  as

$$\mathbf{A}_l \in \mathbb{R}^{C \times H \times W \times Z}, \quad (2)$$

where  $C$ ,  $H$ ,  $W$ , and  $Z$  represent the channels, height, width, and token sequence length, respectively. We then use the  $\{\text{CLS}\}$  token index to select the corresponding cross-attention map, denoted as:

$$\mathbf{A}_l^{\{\text{CLS}\}} \in \mathbb{R}^{C \times H \times W}. \quad (3)$$

To create a consolidated attention map for the  $\{\text{CLS}\}$  token

across a set of layers  $L = \{l_1, l_2, \dots, l_n\}$ , we first concatenate the attention maps from these layers:

$$\mathbf{A}_{\text{concat}}^{\{\text{CLS}\}} = [\mathbf{A}_{l_1}^{\{\text{CLS}\}}, \dots, \mathbf{A}_{l_n}^{\{\text{CLS}\}}] \in \mathbb{R}^{H \times W \times (n \cdot C)}. \quad (4)$$

We then compute the channel-wise mean to obtain a spatial map that localizes the fine-grained objects:

$$\mathbf{A}_{\text{map}}^{\{\text{CLS}\}} = \frac{1}{n \cdot C} \sum_i^{n \cdot C} \mathbf{A}_{\text{concat}}^{\{\text{CLS}\}}[i]. \quad (5)$$

By extracting the cross-attention output for the relevant token and averaging across channels, we generate a spatial attention map that highlights the locations of objects within the fine-grained category. This setup yields a synthetic image  $x^{\text{syn}}$ , a fine-grained category label  $y^{\{\text{CLS}\}}$ , and an attention map  $\mathbf{A}_{\text{map}}^{\{\text{CLS}\}}$  that localizes the fine-grained objects, providing a pseudo-annotation for each generated image.

#### 4.2. Fine-Grained Attention Prediction

To achieve fine-grained localization in densely populated scenes, we train an attention prediction network,  $f_{ag}$ , parameterized by  $\theta$ , which takes an input image  $x$  and outputs a semantic attention map  $\tilde{\mathbf{A}}_{\text{map}}^{\{\text{CLS}\}}$  focused on specific fine-grained categories. This network builds on DinoV2 [20] by fine-tuning a lightweight, fine-grained head on top of frozen DinoV2 image features. Freezing the main feature layers allows us to efficiently leverage DinoV2’s spatial and semantic embeddings without extensive retraining. An overview of this training process is provided in Fig. 6.

To optimize  $\theta$ , we use synthetic images and their corresponding attention maps as pseudo-annotations. Each map is paired with a fine-grained category label  $y^{\{\text{CLS}\}}$  for one of  $N$  categories, providing spatial supervision that guides the network to learn fine-grained distinctions by treating each target category as foreground and all others as background.

For each category  $i$ , let  $\mathbf{A}_{\text{map}}^{\{i\}} \in [0, 1]^{H \times W}$  represent the attention map. We stack these maps to create a multi-channel target map,  $\mathbf{A}_y \in [0, 1]^{N \times H \times W}$ , where each channel corresponds to a different fine-grained category:

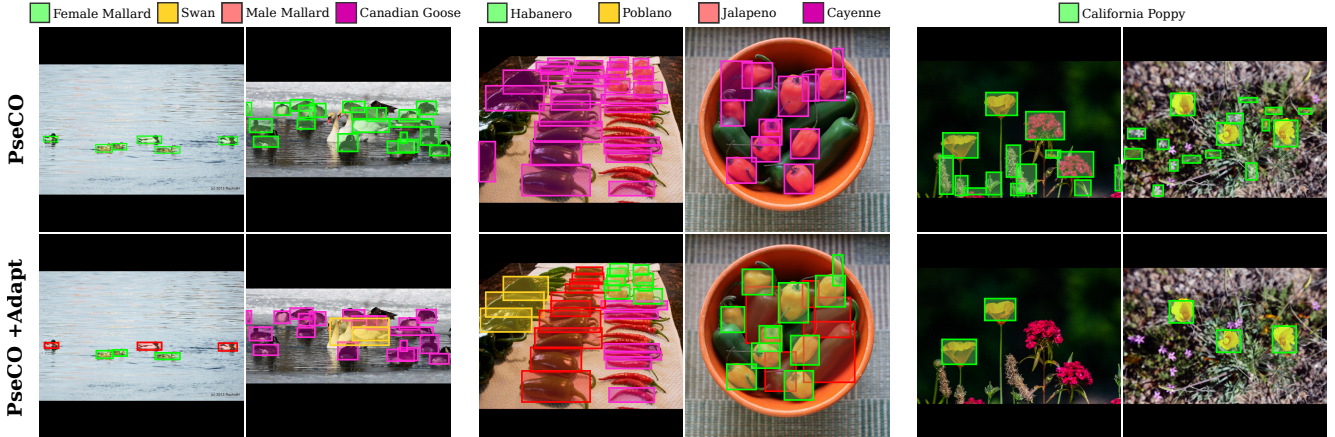


Figure 8. **Qualitative.** Examples from each dataset using PseCO with and without our adaptation. For the baseline, we show one prompt category to illustrate overcounting issues. For our technique, we display all object categories identified by our network. In the wildflowers example, flowers from the ‘Other’ category remain unlabeled.

Method	Waterfowl			Peppers			Wildflowers		
	MAE <sub>all</sub> <sup>c</sup>	MAE <sub>+</sub> <sup>c</sup>	MAE <sub>0</sub> <sup>c</sup>	MAE <sub>all</sub> <sup>c</sup>	MAE <sub>+</sub> <sup>c</sup>	MAE <sub>0</sub> <sup>c</sup>	MAE <sub>all</sub> <sup>c</sup>	MAE <sub>+</sub> <sup>c</sup>	MAE <sub>0</sub> <sup>c</sup>
OwlV2 [17]	9.2	15.8	6.2	23.1	36.3	15.9	11.5	<b>27.5</b>	8.1
Ground. Dino [14]	4.0	7.0	2.3	10.3	16.9	5.0	10.7	34.4	3.6
PseCo [32]	15.3	15.1	15.8	37.2	29.7	41.7	41.3	38.0	41.8
+ Adapt	<b>2.1</b>	<b>5.8</b>	0.3	<b>4.4</b>	<b>9.3</b>	1.7	<b>6.5</b>	28.2	<b>0.6</b>
DAVE [21]	28.2	24.2	29.9	42.5	33.2	49.1	106.1	110.9	117.6
+ Adapt	2.2	6.1	<b>0.2</b>	4.6	10.0	<b>1.2</b>	7.3	28.9	0.9
Baseline	25.1	20.9	26.4	39.8	35.2	43.3	73.1	54.6	79.0
+ Adapt	2.4	6.4	0.3	8.6	17.8	2.5	7.1	29.0	0.9

Table 2. **Results.** Mean absolute error (MAE) results for various methods. ‘‘All’’ denotes overall MAE, ‘‘+’’ is MAE for images with at least one relevant object, and ‘‘0’’ is MAE for images with zero relevant objects. ‘‘Adapt’’ indicates the addition of our contribution.

$$\mathbf{A}_y = [\mathbf{A}_{\text{map}}^{\{1\}}, \mathbf{A}_{\text{map}}^{\{2\}}, \dots, \mathbf{A}_{\text{map}}^{\{N\}}]. \quad (6)$$

Each spatial location  $(h, w)$  in  $\mathbf{A}_y$  reflects the likelihood of that position belonging to a specific category  $i$ , enabling the network to differentiate between the  $N$  fine-grained categories effectively. Although the training images contain only one fine-grained category at a time, the network learns to distinguish between categories when multiple are present in a single image during testing, as demonstrated in Fig. 6.

We train the network by minimizing a cross-entropy loss over the pseudo-labeled attention maps, guiding the network to align its predictions with regions containing each fine-grained category. In Fig. 7, we present examples of fine-grained attention maps generated by our method on real images, applying thresholding to produce binary masks.

### 4.3. Guiding Counting Networks with Attention

Our method extends pre-trained zero-shot and few-shot counting models to support fine-grained category counting.

We denote a pre-trained counting network as:

$$\hat{D} = g_{cnt}(x), \quad (7)$$

where the network  $g_{cnt}$  takes an input image  $x$  and produces a dense object count estimate  $\hat{D}$ , which may be represented as a density map, point estimates, bounding boxes, or other spatial representations of the object count.

Once the fine-grained attention guidance network  $f_{ag}$  is trained, we integrate its predictions with the pre-trained counting network to isolate fine-grained categories. The adapted network for fine-grained counting is then given by:

$$\hat{D}_{fg} = f_{ag} \circ g_{cnt}(x), \quad (8)$$

where the  $i$ -th index of  $\hat{D}_{fg}$  represents the count for the  $i$ -th fine-grained category identified by  $f_{ag}$ . This integration improves counting accuracy in complex scenes and minimizes the need for manual annotations.



Figure 9. **Qualitative Generalization.** Our method demonstrates strong generalizability across diverse fine-grained categories despite high visual similarity within each category, including pasta shapes (penne, fusilli, gnocchi), tomato cultivars (cherry, beefsteak), apple cultivars (Gala, Granny Smith, Red Delicious), gemstone finishes (tumbled, raw), and potato cultivars (Sweet Potato, Yukon Gold).

## 5. Experiments and Results

**Implementation.** We evaluate our method on three zero-shot counting models: (i) a baseline model combining DinoV2 [20] and CLIP [24], trained on FSC147 [25]; (ii) DAVE [21]; and (iii) PseCo [32]. For DAVE and PseCo, we use pre-trained weights to assess performance on FGTC, then adapt them with our attention guidance network. We also test state-of-the-art open-set detection models, Grounding Dino [14] and OwlV2 [17], trained on extensive data for generalized object detection. For each method, we use the full fine-grained category name as the prompt.

To train our attention guidance network, we generate 300 synthetic images per category and 300 background only images. We train the model for 20 epochs with a learning rate of  $5 \times 10^{-5}$  using the AdamW optimizer [15].

**Evaluation Criteria.** We assess all methods using the mean absolute error (MAE) averaged across categories. Specifically, the MAE is defined as

$$\text{MAE}^c = \frac{1}{C} \sum_{c=1}^C \frac{1}{N_c} \sum_{i=1}^{N_c} |y_i^{(c)} - \hat{y}_i^{(c)}|, \quad (9)$$

where  $C$  denotes the number of fine-grained categories,  $N_c$  is the number of images within category  $c$ , and  $y_i^{(c)}$  and  $\hat{y}_i^{(c)}$  represent the true and predicted counts for the  $i$ -th image in category  $c$ , respectively. In addition, we report  $\text{MAE}_+^c$ , the MAE computed over images containing at least one instance of the relevant object, and  $\text{MAE}_0^c$ , the MAE computed over images that do not contain any instances of the relevant object.

**Main Results.** Our method, labeled as “Adapt” in Table Tab. 2, shows significant performance improvements across

all three taxonomic groups. In nearly every case, “Adapt” enhances the baseline model’s accuracy and outperforms open-set detection methods. For example, applying our method to PseCO for the waterfowl set reduces the MAE from 19.6 to 1.9; a 90.3% reduction in error. This highlights our method’s effectiveness in reducing over-counting by focusing on relevant objects within each category.

**Qualitative Results.** In Figure 8, we present qualitative results demonstrating the impact of our method. Pre-trained counting models often overcount when multiple object categories within the same taxonomic group appear, leading to boundary confusion. Our approach improves their ability to distinguish fine-grained categories, reducing overcounting of irrelevant objects. While it does not enhance detection, refining the counting process by filtering out irrelevant categories leads to substantial performance improvements.

**Generalization.** Figure 9 highlights our method’s ability to generalize to other fine-grained categories, demonstrating its capacity to distinguish visually similar objects across diverse domains. We evaluate five categories—pasta shapes, tomato cultivars, apple cultivars, gemstone finishes, and potato cultivars—each containing instances with subtle intra-category variations. Despite these challenges, our method successfully separates these categories, further validating its value for fine-grained counting.

**Comparison to Open-World Segmentation.** In Table 3 and Figure 10, we compare our method against the open-world segmentation methods OVSeg [12] and CLIPSeg [16]. Our method outperforms both on the FGTC dataset, highlighting its effectiveness in reducing false positives in fine-grained counting scenarios. We attribute this



Figure 10. **Qualitative Open-world Segmentation.** We compare our method against open-vocabulary segmentation, demonstrating its ability to accurately localize fine-grained object categories.

Method	Waterfowl		Peppers		Wildflowers	
	MAE <sub>+</sub> <sup>c</sup>	MAE <sub>0</sub> <sup>c</sup>	MAE <sub>+</sub> <sup>c</sup>	MAE <sub>0</sub> <sup>c</sup>	MAE <sub>+</sub> <sup>c</sup>	MAE <sub>0</sub> <sup>c</sup>
CLIPSeg	9.3	3.2	17.8	5.6	37.6	1.4
OVSeg	10.0	6.1	15.7	4.6	81.1	18.8
Ours	<b>6.1</b>	<b>0.2</b>	<b>10.0</b>	<b>1.2</b>	<b>28.9</b>	<b>0.9</b>

Table 3. Comparison to open-vocabulary segmentation methods. Results averaged over categories and each method uses DAVE.

performance gain to the challenges these methods face in distinguishing between visually similar fine-grained objects, as their feature representations lack the necessary disentanglement for fine-grained differentiation. This limitation is exacerbated by the under representation of densely packed fine-grained objects in the datasets used to train open-world segmentation models.

**The Impact of Irrelevant Objects.** A unique aspect of the FGTC dataset is the presence of multiple similar objects per image, which introduces the challenge of distinguishing relevant from irrelevant objects. To evaluate how our attention guidance method performs in such scenarios, we introduce the *Distractor Ratio*, defined as:

$$\text{Distractor Ratio} = \frac{C_{\text{irrel}} - C_{\text{rel}}}{C_{\text{rel}} + C_{\text{irrel}}} \quad (10)$$

where  $C_{\text{rel}}$  is the count of relevant objects and  $C_{\text{irrel}}$  is the count of irrelevant objects. The Distractor Ratio is bounded between -1 and +1 where -1 indicates that all objects are relevant and +1 indicates they are irrelevant.

In Fig. 11, we plot the Relative Absolute Error (rAE),

$$rAE = \left| \frac{y_i - \hat{y}_i}{\hat{y}_i} \right|, \quad (11)$$

against the Distractor Ratio for different object categories using PSeCo as the baseline, focusing on examples with

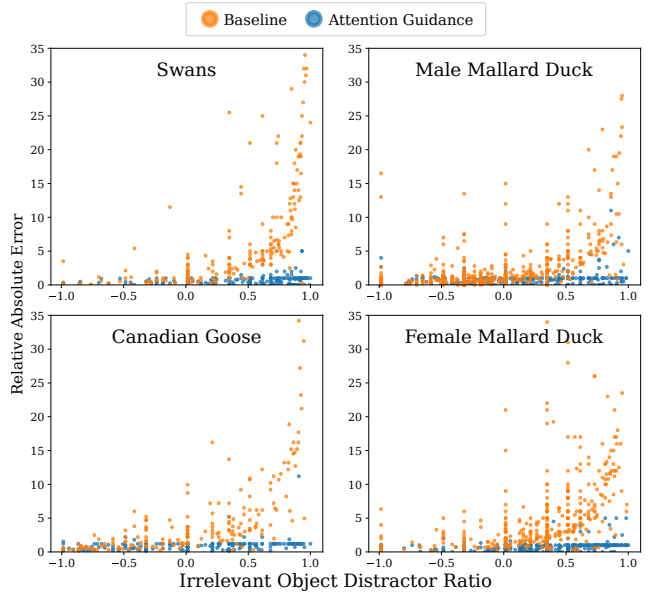


Figure 11. **Impact of Irrelevant Objects.** As irrelevant objects increase, the baseline (PSeCo) suffers sharp error growth, while our method effectively mitigates this impact, improving performance.

at least one relevant object. As the Distractor Ratio approaches +1, baseline error rises sharply due to false positives. However, when our attention guidance method is applied to the baseline output, this error decreases substantially. Notably, even with a Distractor Ratio near +1, where irrelevant objects outnumber relevant ones, performance remains stable (rAE nearly constant), demonstrating that our method effectively mitigates the impact of irrelevant objects and enhances counting accuracy in cluttered scenes.

## 6. Conclusion

We introduced an annotation-free approach for fine-grained object counting using synthetic data and cross-attention maps from latent diffusion models. Our method guides pre-trained counting models to relevant objects in complex scenes, substantially improving accuracy across categories in the FGTC dataset. Evaluations on Waterfowl, Wildflowers, and Pepper Cultivars show reduced over-counting errors, outperforming baseline and open-set methods. This scalable solution minimizes the need for annotated data, expanding applications in fields like ecology and agriculture.

**Limitations.** Although our method performs well on natural images, its effectiveness is constrained by the types of images latent diffusion models can generate. In domains like medical imaging, where image representation is sparse, our approach may be less applicable. Advances such as Break-A-Scene [1], which learn personalized tokens for novel objects, could mitigate this limitation through the addition of new concepts.

## References

- [1] Omri Avrahami, Kfir Aberman, Ohad Fried, Daniel Cohen-Or, and Dani Lischinski. Break-a-scene: Extracting multiple concepts from a single image. In *SIGGRAPH Asia 2023 Conference Papers*, New York, NY, USA, 2023. Association for Computing Machinery. 8
- [2] Liu Chang, Zhong Yujie, Zisserman Andrew, and Xie Weidi. Countr: Transformer-based generalised visual counting. In *British Machine Vision Conference (BMVC)*, 2022. 2
- [3] Omer Dahary, Or Patashnik, Kfir Aberman, and Daniel Cohen-Or. Be yourself: Bounded attention for multi-subject text-to-image generation, 2024. 1
- [4] Siyang Dai, Jun Liu, and Ngai-Man Cheung. Referring expression counting. In *Proceedings of the IEEE/CVF Conference on Computer Vision and Pattern Recognition (CVPR)*, pages 16985–16995, 2024. 3
- [5] Adriano D’Alessandro, Ali Mahdavi-Amiri, and Ghassan Hamarneh. Afreeca: Annotation-free counting for all. In *Computer Vision – ECCV 2024*, pages 75–91, Cham, 2025. Springer Nature Switzerland. 1, 2
- [6] Nikola Djukic, Alan Lukezic, Vitjan Zavrtanik, and Matej Kristan. A low-shot object counting network with iterative prototype adaptation, 2023. 1, 2
- [7] Adriano C. D’Alessandro, Ali Mahdavi-Amiri, and Ghassan Hamarneh. Learning-to-count by learning-to-rank. In *2023 20th Conference on Robots and Vision (CRV)*, pages 105–112, 2023. 2
- [8] Ruifei He, Shuyang Sun, Xin Yu, Chuhui Xue, Wenqing Zhang, Philip Torr, Song Bai, and XIAOJUAN QI. Is synthetic data from generative models ready for image recognition? In *The Eleventh International Conference on Learning Representations (ICLR)*, 2023. 2
- [9] Amir Hertz, Ron Mokady, Jay Tenenbaum, Kfir Aberman, Yael Pritch, and Daniel Cohen-Or. Prompt-to-prompt image editing with cross attention control. 2022. 1
- [10] Lukas Knobel, Tengda Han, and Yuki M. Asano. Learning to count without annotations. In *CVPR*, 2024. 1
- [11] Dingkan Liang, Jiahao Xie, Zhikang Zou, Xiaoqing Ye, Wei Xu, and Xiang Bai. Crowdclip: Unsupervised crowd counting via vision-language model. In *Proceedings of the IEEE/CVF Conference on Computer Vision and Pattern Recognition (CVPR)*, pages 2893–2903, 2023. 2
- [12] F. Liang, B. Wu, X. Dai, K. Li, Y. Zhao, H. Zhang, P. Zhang, P. Vajda, and D. Marculescu. Open-vocabulary semantic segmentation with mask-adapted clip. In *CVPR*, 2023. 7
- [13] Chang Liu, Henghui Ding, and Xudong Jiang. Gres: Generalized referring expression segmentation. In *Proceedings of the IEEE/CVF conference on computer vision and pattern recognition*, pages 23592–23601, 2023. 3
- [14] Shilong Liu, Zhaoyang Zeng, Tianhe Ren, Feng Li, Hao Zhang, Jie Yang, Chunyuan Li, Jianwei Yang, Hang Su, Jun Zhu, et al. Grounding dino: Marrying dino with grounded pre-training for open-set object detection. 2025. 3, 6, 7
- [15] Ilya Loshchilov and Frank Hutter. Decoupled weight decay regularization. In *International Conference on Learning Representations*, 2019. 7
- [16] T. Lüddecke and A. Ecker. Image segmentation using text and image prompts. In *CVPR*, 2022. 7
- [17] Matthias Minderer, Alexey Gritsenko, and Neil Houlsby. Scaling open-vocabulary object detection. *Advances in Neural Information Processing Systems*, 36, 2024. 6, 7
- [18] Anindya Mondal, Sauradip Nag, Xiatian Zhu, and Anjan Dutta. Omnicount: Multi-label object counting with semantic-geometric priors. *arXiv preprint arXiv:2403.05435*, 2024. 1
- [19] Maria-Elena Nilsback and Andrew Zisserman. Automated flower classification over a large number of classes. In *2008 Sixth Indian conference on computer vision, graphics & image processing*, pages 722–729. IEEE, 2008. 3
- [20] Maxime Oquab, Timothée Darcet, Théo Moutakanni, Huy V. Vo, Marc Szafraniec, Vasil Khalidov, Pierre Fernandez, Daniel HAZIZA, Francisco Massa, Alaaeldin El-Nouby, Mido Assran, Nicolas Ballas, Wojciech Galuba, Russell Howes, Po-Yao Huang, Shang-Wen Li, Ishan Misra, Michael Rabbat, Vasu Sharma, Gabriel Synnaeve, Hu Xu, Herve Jegou, Julien Mairal, Patrick Labatut, Armand Joulin, and Piotr Bojanowski. DINOv2: Learning robust visual features without supervision. *Transactions on Machine Learning Research*, 2024. 5, 7
- [21] Jer Pelhan, Alan Lukežič, Vitjan Zavrtanik, and Matej Kristan. Dave - a detect-and-verify paradigm for low-shot counting. In *Proceedings of the IEEE/CVF Conference on Computer Vision and Pattern Recognition (CVPR)*, pages 23293–23302, 2024. 2, 6, 7
- [22] Dustin Podell, Zion English, Kyle Lacey, Andreas Blattmann, Tim Dockhorn, Jonas Müller, Joe Penna, and Robin Rombach. SDXL: Improving latent diffusion models for high-resolution image synthesis. In *The Twelfth International Conference on Learning Representations*, 2024. 1, 5
- [23] Maan Qraitem, Kate Saenko, and Bryan A. Plummer. From fake to real: Pretraining on balanced synthetic images to prevent spurious correlations in image recognition. In *Computer Vision – ECCV 2024*, pages 230–246, Cham, 2025. Springer Nature Switzerland. 2
- [24] Alec Radford, Jong Wook Kim, Chris Hallacy, Aditya Ramesh, Gabriel Goh, Sandhini Agarwal, Girish Sastry, Amanda Askell, Pamela Mishkin, Jack Clark, et al. Learning transferable visual models from natural language supervision. In *International conference on machine learning*, pages 8748–8763. PMLR, 2021. 7
- [25] Viresh Ranjan, Udbhav Sharma, Thu Nguyen, and Minh Hoai. Learning to count everything. In *Proceedings of the IEEE/CVF Conference on Computer Vision and Pattern Recognition (CVPR)*, 2021. 1, 2, 7
- [26] Deepak Babu Sam, Neeraj N Sajjan, Himanshu Maurya, and R Venkatesh Babu. Almost unsupervised learning for dense crowd counting. In *Proceedings of the AAAI Conference on Artificial Intelligence*, pages 8868–8875, 2019. 2
- [27] Jordan Shipard, Arnold Wiliem, Kien Nguyen Thanh, Wei Xiang, and Clinton Fookes. Diversity is definitely needed: Improving model-agnostic zero-shot classification via stable diffusion. In *Proceedings of the IEEE/CVF Conference on*

- Computer Vision and Pattern Recognition*, pages 769–778, 2023. [2](#)
- [28] Khoi Nguyen Thanh Nguyen, Chau Pham and Minh Hoai. Few-shot Object Counting and Detection. In *Proceedings of the European Conference on Computer Vision 2022*, 2022. [1](#), [2](#)
- [29] C. Wah, S. Branson, P. Welinder, P. Perona, and S. Belongie. Caltech-ucsd birds 200. Technical Report CNS-TR-2011-001, California Institute of Technology, 2011. [3](#)
- [30] Chi Xie, Zhao Zhang, Yixuan Wu, Feng Zhu, Rui Zhao, and Shuang Liang. Described object detection: Liberating object detection with flexible expressions. *Advances in Neural Information Processing Systems*, 36, 2024. [3](#)
- [31] Jingyi Xu, Hieu Le, Vu Nguyen, Viresh Ranjan, and Dimitris Samaras. Zero-shot object counting. In *Proceedings of the IEEE/CVF Conference on Computer Vision and Pattern Recognition*, pages 15548–15557, 2023. [1](#), [2](#)
- [32] Huang Zhizhong, Dai Mingliang, Zhang Yi, Zhang Junping, and Shan Hongming. Point, segment and count: A generalized framework for object counting. In *CVPR*, 2024. [6](#), [7](#)
- [33] Huilin Zhu, Jingling Yuan, Zhengwei Yang, Yu Guo, Zheng Wang, Xian Zhong, and Shengfeng He. Zero-shot object counting with good exemplars. In *Computer Vision – ECCV 2024*, pages 368–385, Cham, 2025. Springer Nature Switzerland. [1](#), [2](#)